

## Cytotoxic effects of essential oils from four *Lippia alba* chemotypes in human liver and lung cancer cell lines

Sandra Montero-Villegas, Rosana Crespo, Boris Rodenak-Kladniew, María Agustina Castro, Marianela Galle, José F. Ciccío, Margarita García de Bravo & Mónica Polo

To cite this article: Sandra Montero-Villegas, Rosana Crespo, Boris Rodenak-Kladniew, María Agustina Castro, Marianela Galle, José F. Ciccío, Margarita García de Bravo & Mónica Polo (2018): Cytotoxic effects of essential oils from four *Lippia alba* chemotypes in human liver and lung cancer cell lines, Journal of Essential Oil Research, DOI: [10.1080/10412905.2018.1431966](https://doi.org/10.1080/10412905.2018.1431966)

To link to this article: <https://doi.org/10.1080/10412905.2018.1431966>



Published online: 01 Feb 2018.



Submit your article to this journal [↗](#)



Article views: 5



View related articles [↗](#)



View Crossmark data [↗](#)



## Cytotoxic effects of essential oils from four *Lippia alba* chemotypes in human liver and lung cancer cell lines

Sandra Montero-Villegas<sup>a</sup>, Rosana Crespo<sup>a</sup>, Boris Rodenak-Kladniew<sup>a</sup>, María Agustina Castro<sup>a</sup>, Marianela Galle<sup>a</sup>, José F. Cicció<sup>b</sup>, Margarita García de Bravo<sup>a</sup> and Mónica Polo<sup>a</sup>

<sup>a</sup>Facultad de Ciencias Médicas, Instituto de Investigaciones Bioquímicas de La Plata “Prof. Dr. Rodolfo R. Brenner” (INIBIOLP) UNLP-CONICET CCT La Plata, La Plata, Argentina; <sup>b</sup>Escuela de Química y Centro de Investigaciones en Productos Naturales (CIPRONA), Universidad de Costa Rica, San José, Costa Rica

### ABSTRACT

Essential oils (EOs) from aromatic plants contain molecules that can interfere with diseases such as cancer and are considered attractive because of their widespread use, good bioavailability, low toxicity and affordable cost. EOs from *Lippia alba* (LaEOs) manifest intraspecific chemical differences in its composition – defined as chemotypes – and is notable for the chemical diversity of their volatile secondary metabolites. We evaluated LaEOs chemotypes cytotoxicity on human cancer culture cells and investigated the mechanisms involved in tagetenone (ta) chemotype cytotoxicity. It exhibited selective cytotoxicity against HepG2 and A549 cells. The mechanism involved cell cycle arrest and apoptosis induction. Tagetenone chemotype (LaEOta) treatment caused 3-hydroxy-3-methylglutaryl-coenzyme A reductase decrease and profound cholesterologenesis inhibition with farnesyl pyrophosphate redirection towards other end products, such as ubiquinone. This work contributes to a clearer understanding of mechanisms of action of LaEOta, thus suggesting that the use of that tagetenone chemotype could provide significant health benefits as a chemopreventive and/or chemotherapeutic agent.

### ARTICLE HISTORY

Received 29 March 2017  
Accepted 6 January 2018

### KEYWORDS

*Lippia alba*; cell proliferation; apoptosis; cell cycle arrest; mevalonate pathway; HMGCR

## 1. Introduction

Cancer has emerged as one of the most alarming diseases in the last decades. According to World Health Organization (1), incidence and mortality of cancer is increasing worldwide indicating the deficiency in present cancer therapies.

Currently used drugs for cancer treatment are often associated with the development of multidrug resistance, serious side effects and high cost. Therefore, anticancer agents with higher tumour burden reduction efficacy, fewer side effects and acquired at affordable cost are critically needed (2).

Plants represent a viable alternative because they continue being the major source and inspiration for developing therapeutic agents. The interest in medicinal plant research for cancer treatment has recently increased (2,3).

Among plant-derived compounds, essential oils (EOs) from aromatic plants have been attractive for their widespread use, good bioavailability, low toxicity and economical price (4–6). EOs are complex mixtures of odoriferous substances consisting mostly of hydrophobic chemical

components, diffusing easily across cell membranes and then inducing biological reactions through which a wide variety of bioactivities including anticancer action is exerted (4–6). The anticancer potential of EOs and their components have been recently published by several authors (7–10).

Indeed, EO biological activity is related to the chemical composition of its main components. Monoterpenes are the most abundant constituents, and antitumour activity of EOs has often been related to the presence those terpenoids in phytocomplex (8,11,12).

An intervention in several biochemical processes has been proposed to explain the anticancer effects of EOs and their constituents (9). Multiple inhibitory effects exercised by monoterpenes on mevalonate pathway (MP) are among those interactions (13–16). MP is a metabolic route where various intermediates and end products are generated with key roles in cell growth, migration, survival and differentiation in mammalian cells (17,18). The main regulation point in MP is catalysed by 3-hydroxy-3-methylglutaryl-coenzyme A reductase (HMGCR), its inhibition

may constitute an effective strategy to reduce malignant cell growth.

*Lippia alba* (Mill.) N.E. Brown is a common aromatic shrub belonging to the Verbenaceae family, present in the Americas, ranging from subtropical regions of North America (northern Mexico and Texas) and the Neotropics (dry forests of Central America or in humid regions of the Caribbean Islands and the Amazon Rainforest in South America) to subtropical regions of the Southern Cone (Argentina, Brazil, and Uruguay). This species is of great interest for its various medicinal uses, especially against digestive disorders and as a sedative remedy (19,20).

*Lippia alba* essential oil (LaEO) is notable for the chemical diversity of volatile secondary metabolites. Monoterpenes – namely myrcene, limonene, 1,8-cineole, linalool, citral (mixture of geranial and neral), carvone and tagetenone (mixture of myrcenone and two isomeric ocimenones) – are frequently found (21). Also, according to environmental and habitat conditions, *L. alba* species may exhibit intraspecific chemical differences in EO composition defined as chemotypes (19,20). Natural variability of chemical composition of essential oils might have significant influence on biological activities and thus possible therapeutic effects (19,20). The cytotoxicity of various LaEO chemotypes, and of some major components, to several tumour cell lines – has been demonstrated (22,23). Nevertheless, those studies still presented only preliminary screening data and therefore did not describe any definitive mechanism of action.

We herein investigated cytotoxicity of four LaEO chemotypes in human liver carcinoma (HepG2), human lung carcinoma (A549) and Vero cells aiming to test their possible use as alternative agents for cancer therapy. Some cytotoxicity-involved mechanisms of LaEO to cancer cells were also evaluated.

## 2. Experimental part

### 2.1. Plant material

Leaves were collected from four *L. alba* chemotypes (carvone, piperitone, tagetenone, and citral) cultivated in Costa Rica. The *L. alba* carvone (plants originally from Costa Rica) and piperitone chemotypes (plants originally from Argentina) were cultivated in the wet tropic of Bougainvillea S. A., in Baltimore, Matina (10°01'03"N, 83°19'41"W), Province of Limón. The *L. alba* tagetenone and citral chemotypes (plants originally from Costa Rica) were cultivated in a private garden in San Rafael de Montes de Oca (9°56'37"N, 84°01'01"W), near San José city in the Central Valley, Province of San José. The plants were identified by R. Ocampo and J. F. Cicció, University of Costa Rica. A voucher specimens were deposited in the

Herbarium of the University of Costa Rica (*L. alba* carvone chemotype: USJ 70741, *L. alba* piperitone chemotype: USJ 93918, *L. alba* tagetenone chemotype: USJ 70698, and *L. alba* citral chemotype: USJ 100626).

### 2.2. Essential oils extraction and analyses

#### 2.2.1. Oil extraction

Dried leaves were hydrodistilled at atmospheric pressure, for 3 h, using a Clevenger-type apparatus. The essential oils were collected and dried over anhydrous sodium sulphate, filtered and stored at 4–10 °C in the dark, for further analysis. The oil yields from diverse chemotypes were: *L. alba* carvone (ca), 1.8% (v/w); *L. alba* (pi), 0.4%; *L. alba* tagetenone (ta), 0.8%, and *L. alba* citral (ci), 0.9%. Extractions were performed in triplicate.

#### 2.2.2. Gas chromatography analyses

The essential oils were analysed by gas chromatography with flame ionization detector (GC-FID) and gas chromatography–mass spectrometry (GC-MS) according to Chaverri and Cicció (24). Briefly, the analytical GC was carried out on a Shimadzu GC-2014 gas chromatograph and the data were obtained on a poly (5% phenyl-95% methylsiloxane) fused silica capillary column (30 m × 0.25 mm; film thickness 0.25 µm), (MDN-5S, Supelco), with a Shimadzu GCsolution™ Chromatography Data System software, version 2.3. Operating conditions were: carrier gas N<sub>2</sub>, flow 1.0 mL/min; oven temperature program: 60–280 °C at 3 °C/min, 280 °C (2 min); sample injection port temperature 250 °C; detector temperature 280 °C; split 1:60. The percentages of the constituents were calculated by electronic integration of FID peak areas without the use of response factor correction.

#### 2.2.3. GC-MS analyses

GC-MS analyses were performed with a Shimadzu GC-17A gas chromatograph coupled with a GCMS-QP5000 apparatus and with GCMSsolution™ software (version 1.21), with Wiley 139 and NIST computerized databases. The analyses were carried out with the same column described above. Operating conditions were: carrier gas He, flow 1.0 mL/min; oven temperature programme: 60–280 °C at 3 °C/min; sample injection port temperature 250 °C; detector temperature 260 °C; ionization voltage: 70 eV; ionization current 60 µA; scanning speed 0.5 s over 38–400 amu range; split 1:70.

#### 2.2.4. Compound identification

The oil constituents were identified using the retention indices (RI) on DB-5 type column (25) and by comparison of their mass spectra with those published in the literature (26) or those of the author's database. To obtain the

retention indices for each peak, 0.1  $\mu\text{L}$  of *n*-alkane mixture ( $\text{C}_8\text{--C}_{32}$ ) was co-injected under the same experimental conditions reported above.

### 2.3. Cell lines, cultivation and treatment conditions

Human liver carcinoma (HepG2), human lung carcinoma (A549) and the noncancerous African green monkey kidney (Vero) cell lines used in this study and obtained from the American Type Culture Collection were cultured in filter-sterilized Eagle's Minimum Essential Medium (MEM; Gibco, Invitrogen Corporation, California, USA) supplemented with 10% (v/v) fetal bovine serum (FBS; Natocor, Córdoba, Argentina) and 100 U/mL penicillin and streptomycin (Richet, Argentina) and were maintained at 37 °C in an atmosphere of 5%  $\text{CO}_2$ -air.

Since the cell lines employed in the present study had different proliferation rates, the number of cultured cells used in the assays was adjusted to a density such that the cells reached the exponential growth phase before starting the experimental incubations and then remained in that phase during the entire treatment. HepG2, A549 and Vero cells were accordingly seeded at densities of 20,000, 10,000 and 45,000 cells/ $\text{cm}^2$ , respectively, and grown under standard conditions for 24 h before changing the medium to fresh medium containing various concentrations of EOs dissolved in dimethyl sulphoxide (DMSO, final concentration 0.2% [v/v]). Control cells were treated with the equivalent amount of the DMSO vehicle.

In the experiments with Mv, cells were treated with EO plus 0.5 mmol/L Mv (Sigma–Aldrich, St. Louis, MO, USA) for 48 h under the above conditions.

For cell treatments with simvastatin (Sv; Merck, Sharp and Dohme, Argentina), the drug was added to the culture medium as the sodium salt in aqueous solution at the indicated concentrations for 48 h (27).

## 2.4. Cell viability and cell proliferation

### 2.4.1. MTT assay

The malignant human cell lines (HepG2 and A549) and the noncancerous cell line (Vero) were seeded in 24-well plates and treated with increasing concentrations of an EO. After treatment, cell viability was tested by the 3-(4,5-dimethylthiazol-2-yl)-2,5-diphenyltetrazolium bromide (MTT) assay according to Crespo (14). All experiments were repeated at least three times.

The phytochemical effect on cell viability was quantified as the percentage of control absorbance. The concentration that reduced cell viability by 50% (the  $\text{IC}_{50}$ ) was obtained by nonlinear regression and is used as the cytotoxicity analysis parameter.

Accordingly, in the experiments the concentrations of the chemotypes will be expressed as multiples or fractions of the respective  $\text{IC}_{50}$  value followed by an '×'. Therefore, to convert this notation into absolute concentration units, the respective  $\text{IC}_{50}$  values listed in Table 2 must be substituted.

The selectivity index (SI) was calculated as the ratio of the  $\text{IC}_{50}$  for the Vero cells divided by the  $\text{IC}_{50}$  for the HepG2 or A549 cells. The SI value indicates the degree of selective toxicity of a given EO to the cancerous cell lines tested relative to that of the nonmalignant line. Any sample of an SI value higher than 3 was considered to have a high selectivity (28).

### 2.4.2. Viable cell count assay

To confirm the results of the MTT assay, cell proliferation was assessed by cell counting using the Trypan blue dye exclusion test to differentiate live and dead cells. Human tumour cells seeded in six-well microtest plates were treated with increasing concentrations of EO. The cells were harvested by trypsinization, the cell suspensions mixed (1/1, v/v) with 0.4% (w/v) trypan blue solution, and cells that excluded Trypan blue counted in a Neubauer chamber. Results are expressed as percentage of viable cells for each concentration tested in comparison to control treatment.

## 2.5. Cell cycle analysis

HepG2 and A549 cells were seeded and treated in 25  $\text{cm}^2$  culture flasks. After treatment, the cell distribution among the different stages of the cell cycle was determined by flow cytometry as previously described (14). Ten thousand events were evaluated per experiment and cellular debris was omitted from the analysis.

## 2.6. Assay of nuclear morphology

Nuclear morphology was visualized by DNA staining with Hoechst 33342 (Sigma–Aldrich, St. Louis, MO, USA) and propidium iodide (PI). HepG2 cells were seeded and treated on cover slips placed in six-well plates. Medium with 3% (v/v) DMSO was used as the positive control for apoptosis. After treatment, the cells were washed with phosphate-buffered saline (PBS: NaCl 137 mM; KCl 2.7 mM, 10.0 mM  $\text{Na}_2\text{HPO}_4$ , 2.0 mM  $\text{KH}_2\text{PO}_4$ , pH 7.4), stained with 5  $\mu\text{g}/\text{mL}$  Hoechst 33342 in PBS in the dark for 20 min at 37 °C, counterstained with 25  $\mu\text{g}/\text{mL}$  PI in PBS in the dark for 15 min at 4 °C and finally washed three times with PBS. The samples were observed under an Olympus BX51 fluorescence microscope (Tokyo, Japan) equipped with an Olympus DP70 digital camera. The microscopical fields were photographed, and merged



images (with blue and red fluorescence) were analysed through the use of ImagePro Plus v. 5.1 software (Media Cybernetics, Silver Spring, Md.).

A total of at least 200 cells were counted and classified into the following four cellular states according to the Hoechst 33342-PI labelling observed (29): LN, live cells with normal nuclei LA, live cells with apoptotic nuclei; DN, dead cells with normal nuclei; and DA, dead cells with apoptotic nuclei. Small elements corresponding to apoptotic bodies were expressly noted and disregarded in the cell counting so as not to overestimate the number of apoptotic cells. The experiment was conducted in triplicate.

The percentages of apoptotic cells were determined according to the following formula:

$$\text{Percentage of apoptotic cells} = \frac{\text{LA} + \text{DA}}{\text{LN} + \text{LA} + \text{DA} + \text{DN}} \times 100$$

### 2.7. *In situ* detection of apoptosis – the TUNEL assay

HepG2 and A549 cells were seeded and treated on coverslips placed in six-well plates. The cells undergoing apoptosis after treatment with EO were identified through the use of the terminal deoxynucleotidyl transferase dUTP nick end labelling (TUNEL) reaction carried out with the *in situ* cell death detection kit with TMR red as the fluorescent marker for labelling dUTP (Roche, Mannheim, Germany) according to the manufacturer's protocol. The TUNEL positive cells were evaluated under a fluorescence microscope (Olympus BX51) and the results analysed by means of the software described above. The cells were counted in 10 random fields with 300 cells each in 3 individual experiments. The results were expressed as the per cent of TUNEL positive cells relative to the total number of cells, the latter being determined by uptake of the fluorescent dye DAPI (4',6-diamidino-2-phenylindole dihydrochloride; Invitrogen by Life Technologies, California, USA).

### 2.8. Incorporation of [<sup>14</sup>C]acetate into nonsaponifiable lipids

HepG2 and A549 cells were seeded in six-well plates and treated as described above before the addition of 2 μCi/mL [<sup>14</sup>C]acetate (56.8 Ci/mol; Perkin Elmer Life Science, Inc.; Boston; MA) for the final 3 h. The nonsaponifiable lipids were then extracted, separated and identified as previously reported (27). After separation by thin-layer chromatography (TLC), all the lipid classes were identified by comparison with a standard mixture containing cholesterol, lanosterol, dolichol, ubiquinone and squalene.

### 2.9. Free and esterified cholesterol content

HepG2 and A549 cells were seeded in culture flasks and treated as described above. The total lipids were extracted

and, free and esterified cholesterol separated by TLC on silicagel G according to Kladniew (27). The quantification was made by means of a curve constructed with pure standards by means of a curve constructed with pure standards that had been run on the same TLC plate. The spot images were analysed by the Image J program.

### 2.10. HMGR levels (Western blotting)

HepG2 cells were seeded and treated in 25-cm<sup>2</sup> flasks. After treatment, the cells were harvested by scraping and HMGR levels were determined by Western blotting as previously described (27). Sv at 5 μM was used as a positive control for increased HMGR levels since the inhibition of the enzyme by the drug results in a compensatory *de novo* synthesis of the HMGR protein.

### 2.11. Statistical analysis

Experimental data were expressed as the means ± SD. Statistical analysis was performed through the use of the one-way analysis of variance (ANOVA) and the Tukey–Kramer multiple-comparisons test with the significance level set at  $p < 0.05$  or else the unpaired Student *t*-test. (GraphPad InStat program). The IC<sub>50</sub> values for cell viability after exposure to the EOs were calculated from the MTT results by nonlinear-regression curves (SigmaPlot software; Systat Software, Inc., Point Richmond, CA). The Selective Index for the two tumour cell lines was calculated against the noncancerous cell line (Vero) from the IC<sub>50</sub> values obtained for all three of the MTT results.

## 3. Results

### 3.1. Chemical composition of LaEO chemotypes cultivated in Costa Rica

Among the compounds identified in the leaf oil, five main classes could be distinguished: monoterpene hydrocarbons, oxygenated monoterpenes, sesquiterpene hydrocarbons, oxygenated sesquiterpenes and the aliphatic 6-methyl-5-hepten-2-one. Table 1 lists the chemical compositions of the LaEOs from the carvone (ca), piperitone (pi), tagetenone (ta) and citral (ci) chemotypes. The main constituents of the leaf oils were oxygenated monoterpenes with a yield of over 50% in all instances.

### 3.2. Cytotoxicity of LaEO chemotypes to cancerous and nonmalignant cells

In order to analyse cytotoxicity, cells were treated with increasing concentrations of EOs and the viability determined by the MTT assay. Table 2 shows the IC<sub>50</sub> values obtained from concentration to viability plots for the

Table 1. Percentage composition of the essential oils of *Lippia alba* chemotypes.

Compound <sup>a</sup>	RI <sup>b</sup>	Lit. RI <sup>c</sup>	IM <sup>d</sup>	ca	Chemotype <sup>e</sup>				
					pi	ta	ci	ta	ci
<i>Monoterpene hydrocarbons</i>									
α-Pinene	936	932	1, 2, 3	-	-	-	0.6	-	-
Sabinene	971	969	1, 2	-	-	-	4.3	-	-
Myrcene	990	988	1, 2	0.2	0.1	0.1	11.0	0.1	0.1
Limonene	1024	1024	1, 2, 3	13.6	9.0	9.0	2.0	0.4	0.4
(E)-β-Ocimene	1049	1044	1, 2	0.1	0.1	0.1	1.9	0.2	0.2
<i>Oxygenated monoterpenes</i>									
1,8-cineole	1033	1026	1, 2, 3	-	-	-	21.4	-	-
Linalool	1096	1095	1, 2	0.5	0.4	0.4	1.4	1.6	1.6
Myrcenone	1147	1145	1, 2	-	-	-	20.6	-	-
Citronellal	1157	1148	1, 2, 3	-	-	-	-	0.8	0.8
Borneol	1165	1165	1, 2	0.5	-	-	0.5	0.2	0.2
trans-Dihydrocarvone	1200	1200	1, 2	0.2	-	-	-	-	-
Nerol	1229	1227	1, 2	-	-	-	-	3.5	3.5
Neral	1235	1235	1, 2, 3	-	-	-	-	14.1	14.1
(Z)-Ocimenone	1229	1226	1, 2	-	-	-	7.1	-	-
(E)-Ocimenone	1238	1235	1, 2	-	-	-	11.7	-	-
Carvone	1244	1239	1, 2, 3	58.6	0.2	0.2	-	-	-
Geraniol	1252	1249	1, 2	-	-	-	-	17.6	17.6
Piperitone	1253	1249	1, 2	1.5	52.4	-	1.9	-	-
Geranial	1267	1264	1, 2	-	-	-	-	22.9	22.9
Piperitenone	1343	1340	1, 2	3.0	0.8	0.8	-	-	-
<i>Sesquiterpenes hydrocarbons</i>									
β-Bourbonene	1388	1387	1, 2	1.0	0.5	0.5	0.1	-	-
β-Cubebene	1384	1387	1, 2	0.1	0.2	0.2	0.2	0.2	0.2
β-Elementene	1389	1389	1, 2	0.7	0.3	0.3	0.9	1.6	1.6
β-Caryophyllene	1421	1417	1, 2, 3	0.3	3.0	3.0	0.9	3.7	3.7
(Z)-β-Farnesene	1442	1440	1, 2	0.6	-	-	-	-	-
α-Humulene	1453	1452	1, 2	-	0.2	0.2	-	0.4	0.4
Germacrene-D	1484	1484	1, 2	10.1	1.9	1.9	3.2	4.2	4.2
Bicyclogermacrene	1505	1500	1, 2	0.6	-	-	-	0.2	0.2
α-Murolene	1507	1500	1, 2	0.1	3.1	3.1	-	0.2	0.2
Germacrene A	1511	1508	1, 2	0.3	-	-	-	0.6	0.6
δ-Cadinene	1525	1522	1, 2	0.1	4.1	4.1	-	-	-
<i>Oxygenated sesquiterpenes</i>									
Neryl acetate	1361	1359	1, 2	-	-	-	-	0.3	0.3
Geranyl acetate	1381	1379	1, 2	-	-	-	-	2.5	2.5
epi-Cubebol	1494	1493	1, 2	-	0.5	0.5	-	-	-
Cubebol	1519	1514	1, 2	0.7	-	-	-	-	-
Hedycaryl	1548	1546	1, 2	-	-	-	4.2	-	-
Germacrene D-4-ol	1570	1574	1, 2	0.4	-	-	0.4	-	-
Caryophyllene oxide	1590	1582	1, 2	-	-	-	-	1.2	1.2
epi-α-Murolol	1642	1640	1, 2	-	-	-	-	-	-
α-Cadinol	1652	1652	1, 2	-	-	-	-	-	-
<i>Aliphatics</i>									
6-Methyl-5-hepten-2-one	982	981	1, 2	-	-	-	-	12.5	12.5
Total				93.2	91.8	91.8	94.3	89.0	89.0

<sup>a</sup>Compounds listed in order of elution from MDN-5S column.  
<sup>b</sup>Experimentally determined retention indices relative to C<sub>8</sub>-C<sub>32</sub> n-alkanes.  
<sup>c</sup>Literature retention indices (26).  
<sup>d</sup>Identification method: 1 = retention index, 2 = MS spectra, 3 = standard.  
<sup>e</sup>Chemotypes: carvone, ca; piperitone, pi; tagetenone, ta; and citral, ci.

**Table 2.** IC<sub>50</sub> values of essential oil chemotypes from *Lippia alba* for all three cell lines and the selectivity index with respect to the cancer cell lines.

Cell lines	IC <sub>50</sub> <sup>a</sup> (SI) <sup>b</sup>			
	LaEOca	LaEOpi	LaEOta	LaEOci
HepG2	347.2 ± 28.3 (1.3)	412.2 ± 30.8 (1.4)	33.6 ± 4.0 (6.7)	34.4 ± 3.1 (2.6)
A549	275.2 ± 18.7 (1.6)	304.4 ± 23.7 (1.9)	30.4 ± 3.2 (7.4)	36.1 ± 3.4 (2.5)
Vero	452.1 ± 37.4	592.3 ± 41.5	225.6 ± 15.2	88.8 ± 7.8

Notes: LaEOca = essential oil carvona chemotypes from *Lippia alba*; LaEOpi = essential oil piperitona chemotypes from *Lippia alba*; LaEOta = essential oil tagetenona chemotypes from *Lippia alba*; LaEOci = essential oil citral chemotypes from *Lippia alba*.

<sup>a</sup>IC<sub>50</sub> values (µg/mL) obtained from nonlinear-regression analysis of dose-response viability curves. Values are expressed as the means ± SD, as determined from the results of the MTT assay in triplicate experiments.

<sup>b</sup>SI refers to the selectivity index, calculated as the ratio of IC<sub>50</sub> for Vero cells / cancer-cell lines: an SI value > 3 accordingly indicates high selectivity.

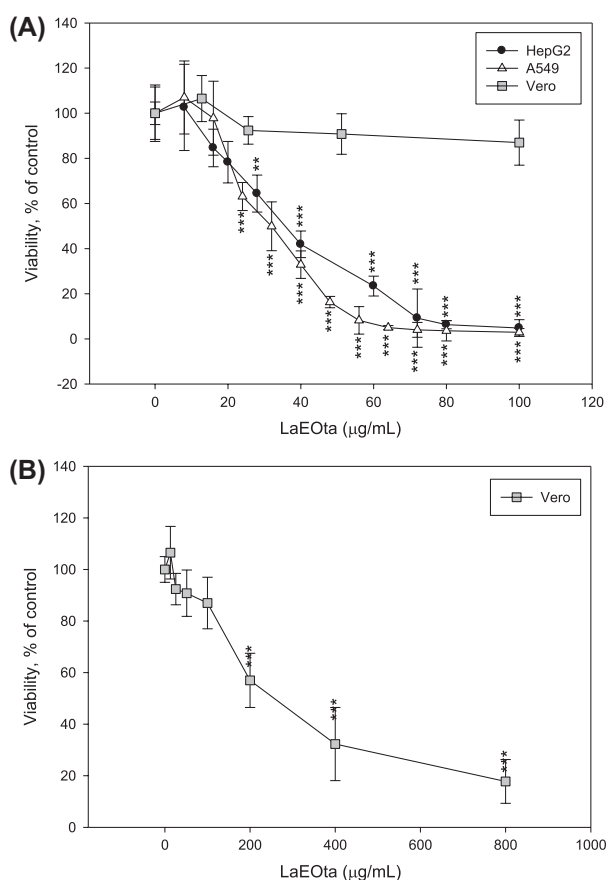


**Figure 1.** Effect of LaEOta on cell viability in human cancer cell lines (HepG2 and A549) and a noncancerous cell line (Vero). Cell viability is expressed as a per cent of the untreated control value. Panel A: LaEOta concentration range producing a selective decrease in the viability of the tumour cell lines; Panel B: extended LaEOta concentration range producing a decrease in the viability of the noncancerous Vero cells. Data are the means ± SD of three independent experiments performed in at least triplicate; \* $p < 0.05$ , \*\* $p < 0.01$ , \*\*\* $p < 0.001$ .

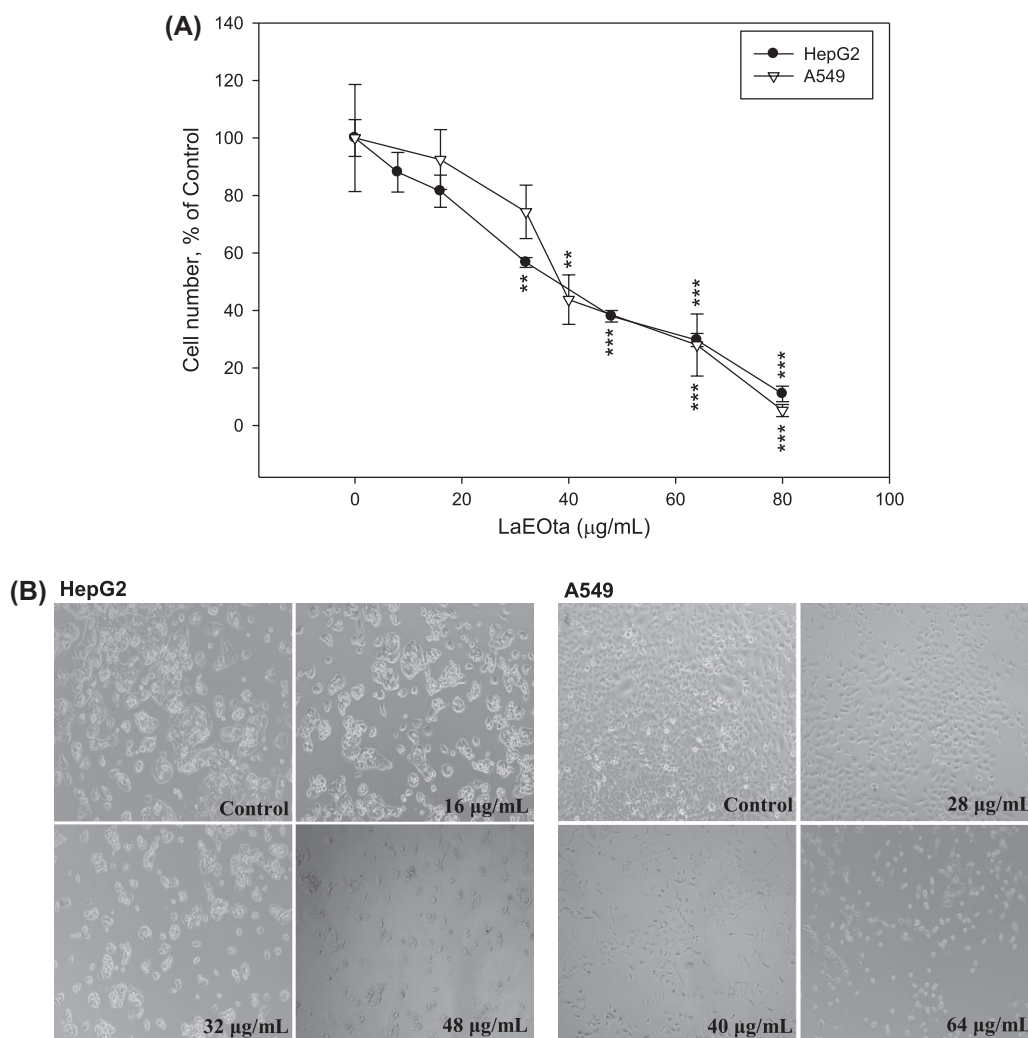
normal and tumour cell lines treated with each one of the EOs extracted from the *L. alba* chemotypes. LaEOs from the citral and tagetenone chemotypes are the most efficient in reducing the viability of HepG2 and A549 carcinoma cells, where the sensitivity (vulnerability) of both tumour cell lines to the oils' cytotoxicity was similar. Although, the IC<sub>50</sub> values in the noncancerous cell line Vero were higher than in the tumour cells for all the oils tested, only the tagetenone chemotype presented a high selectivity (SI > 3) for both tumour cell lines.

Figure 1 shows representative curves of cell viability in response to treatment with increasing concentrations of LaEOta, the most efficient and selective chemotype. In both tumour cell lines, treatments with up to 80 µg/mL of LaEOta produced a progressive dose-dependent decrease in cell viability. Thereafter, the curve plateaued at an inhibition of viability greater than 95% up to the maximum concentration tested in the MTT assay (100 µg/mL; Figure 1(A)). In the Vero nontumour line, LaEOta did not produce a statistically significant inhibition of cell viability within the concentration range tested for the malignant cells. From a concentration of 200 µg/mL on, however, exposure to LaEOta resulted in a dose-dependent decrease in the viability the Vero cells as well (Figure 1(B)), reaching a value of 82% at the highest concentration tested (800 µg/mL).

### 3.3. Antiproliferative activity of LaEOta in human liver and lung carcinoma cells

To confirm the results of the effect of LaEOta – the chemotype with the lowest IC<sub>50</sub> and highest SI according MTT assay – on cancer cells proliferation, HepG2 and A549 cells were treated with progressive LaEOta concentrations (0–80 µg/mL) for 48 h and the total number of viable cells counted. Exposure of HepG2 and A549 cells to LaEOta within this concentration range reduced cell proliferation of the two lines in a dose-dependent manner (Figure 2(A)), with concentrations of 36 and 40 µg/mL inhibiting the proliferation of these liver and lung carcinoma model lines by 50%, respectively.

Photomicrographs in Figure 2(B) illustrate the morphologic changes accompanying the concentration-dependent suppression of proliferation produced in both cell lines after treatment with LaEOta for 48 h. In the absence of LaEOta, HepG2 cells exhibited their typical epithelial morphology and normal trabecular growth. Treatment with LaEOta at 16 µg/mL caused vacuolation and the loss of that trabecular organization, resulting in the presence of cells that were isolated and more rounded up. In cells treated with higher concentrations, these morphologic features increased along with the formation of cells with marked cytoplasmic vacuolization, chromatin



**Figure 2.** Inhibition of proliferation of HepG2 and A549 carcinoma cells after treatment with LaEOta. Panel A: The cell numbers are expressed as percentages of the cells in the untreated control cultures. Data are the means  $\pm$  SD,  $n = 4$ ; \* $p < 0.05$ , \*\* $p < 0.01$ , \*\*\* $p < 0.001$ . Panel B: Photomicrographs of human carcinoma cells following a 48-h treatment with the progressive concentrations of LaEOta indicated in the lower right-hand corner of each field.

condensation and plasma-membrane blebbing, changes reminiscent of apoptosis-induced cell death.

The normal epithelial morphology of the untreated A549 cells was also evident. Exposure to LaEOta at 28  $\mu\text{g/mL}$  caused a reduction in cell volume and the acquisition of a spindle-shaped morphology. A higher concentration (40  $\mu\text{g/mL}$ ) produced cytoplasmic vacuolation and condensation of the cell chromatin, changes reminiscent of cells dying through apoptosis, as was observed in the HepG2 cultures. Upon treatment with an oil concentration that inhibited the proliferation by over 70% (that is, 64  $\mu\text{g/mL}$ ), along with the morphologic changes at the lower oil levels, the cells also became rounded up with some detaching from the growing surface.

### 3.4. Effect of LaEOta on cell cycle progression

Proliferating cells require cell cycle progression from the initial postmitotic G1 phase through S and G2 into M for

a subsequent mitosis. In order to determine if the antiproliferative effects of LaEOta were associated with changes in cell cycle distribution, we treated the HepG2 and A549 carcinoma cells with 0.5 $\times$  and 1.0 $\times$   $\text{IC}_{50}$  concentrations of LaEOta for 48 h and then analysed PI-stained cells in a flow cytometer (Figure 3).

In HepG2 cells (Figure 3(A)), following a 48-h incubation with LaEOta, the percentage of cells in the G1 phase increased, especially at the concentration 1.0 $\times$   $\text{IC}_{50}$  LaEOta. Conversely, the percentage of cells in the S phase decreased. Thus, the G1/S ratio, an indicator of G1 arrest, became elevated from  $1.1 \pm 0.1$  (control) to  $1.8 \pm 0.2$  (at 0.5 $\times$   $\text{IC}_{50}$  LaEOta,  $p < 0.001$ ) and  $2.9 \pm 0.4$  (at 1.0 $\times$   $\text{IC}_{50}$  LaEOta,  $p < 0.001$ ).

LaEOta had a different effect of on the cell cycle distribution in A549 cells (Figure 3(B)). Following a 48-h incubation with 0.5 $\times$   $\text{IC}_{50}$  LaEOta, the percentage of cells in the G1 and S phase and the resulting G1/S ratio did not change significantly; whereas exposure to 1.0 $\times$   $\text{IC}_{50}$



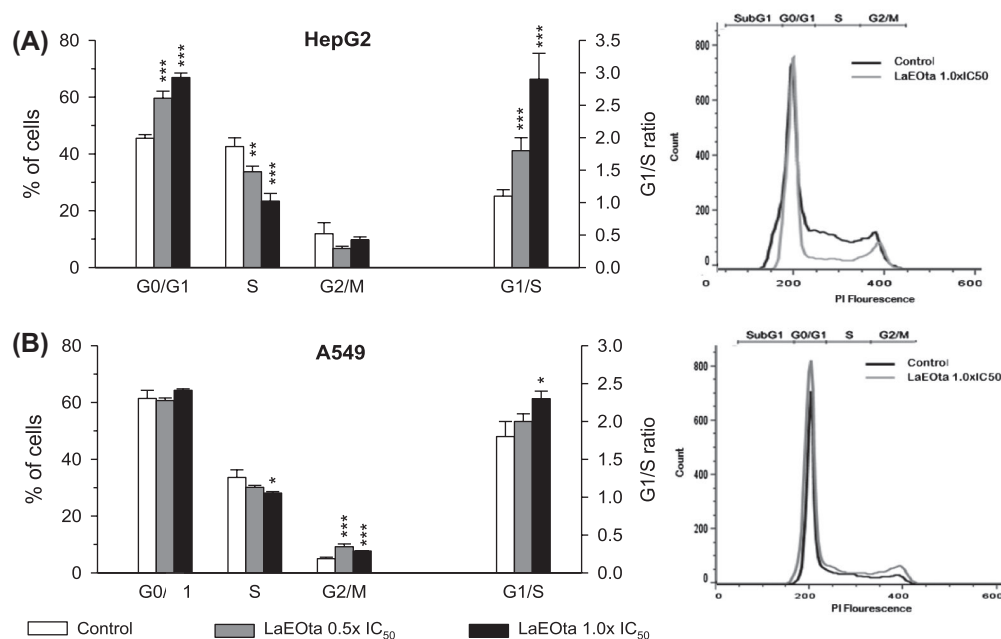


**Figure 3.** Cell cycle analysis of HepG2 (Panel A) and A549 (Panel B) carcinoma cells after treatment with LaEOta for 48 h. In the left-hand figures of each panel, the per cent distribution of each phase of the mitotic cycle indicated on the abscissa is plotted on the left ordinate, while the ratio of the G1- over the S-phase per cent distributions is plotted on the right ordinate. The bars represent the means  $\pm$  SD ( $n = 3$ ). \* $p < 0.05$ , \*\* $p < 0.01$ , \*\*\* $p < 0.001$  vs. control. The right-hand profiles are representative flow cytometry records illustrating the typical differences in the curves obtained between the control (light lines) and experimental (dark lines) groups.

LaEOta decreased the percentage of cells in the S phase while also elevating the percentage of the G1-phase cells, thus causing a significant increase ( $p < 0.05$ ) in the G1/S ratio from  $1.8 \pm 0.2$  (control) to  $2.3 \pm 0.1$  (at  $1.0 \times IC_{50}$  LaEOta). Concomitantly, the percentage of cells in the G2 phase increased from  $5.0 \pm 0.5\%$  (control) to  $9.2 \pm 1.0\%$  (at  $0.5 \times IC_{50}$  LaEOta,  $p < 0.001$ ) and to  $7.7 \pm 0.1\%$  (at  $1.0 \times IC_{50}$  LaEOta,  $p < 0.001$ ), thus suggesting a LaEOta-mediated G2-phase arrest.

### 3.5. Apoptosis induced by LaEOta

According to the cytotoxicity data, both carcinoma cell lines (HepG2 and A549) were sensitive to the cytotoxic effects of LaEOta. Having noted that the morphologic changes in LaEOta-treated cells resembled apoptosis (Figure 2), we therefore investigated whether the mechanism of action of LaEOta against the malignant cell lines involved the involvement of apoptosis.

Apoptosis in HepG2 cells was assayed cytologically by means of double staining with Hoechst 33342 and PI. Cells were incubated with or without LaEOta ( $1.0 \times IC_{50}$ ) for 48 h before the assessment of apoptosis and the determination of morphologic changes in the cell nuclei by fluorescence microscopy.

As observed in Figure 4(A), most of the control cells exhibited intact nuclei of ovoid shape stained with a moderately bright blue fluorescence (from the Hoechst 33342

dye), nuclear components distributed evenly, apparently intact genomic DNA, and the absence of red fluorescence (from the lack of penetration of the PI dye), which pattern denotes intact normal cells. After exposure to LaEOta, numerous cells exhibited features typical of apoptosis. The apoptotic nuclei clearly contained a highly condensed or fragmented chromatin that was uniformly Hoechst 33342 fluorescent. In the cells at the beginning of apoptosis, the membrane permeability was still conserved and the red fluorescence was therefore absent; whereas, the cells late in apoptosis emitted a red fluorescence because the membrane integrity had been compromised and the PI had entered the cells (Figure 4(A), subfields 1 and 2). An increase in cells that emitted a red fluorescence with intact nuclei and organized chromatin – that is, dead cells with normal nuclei – as well as necrotic cells are also observed (Figure 4(A), subfield 2).

Figure 4(B) shows the percentages of apoptotic cells calculated as described in Materials and Methods and summarized in the legend to the figure. The treatment of HepG2 cells with  $1.0 \times IC_{50}$  LaEOta increased the percentage of apoptotic cells by more than fivefold.

To confirm this preliminary indication of the induction of apoptosis by LaEOta in the HepG2 and A549 cells treated with  $1.0 \times IC_{50}$  of LaEOta for 48 h, we conducted the TUNEL assay on cultures incubated under the same conditions. The data obtained demonstrated that the exposure of HepG2 and A549 cells to  $1.0 \times IC_{50}$  of LaEOta caused

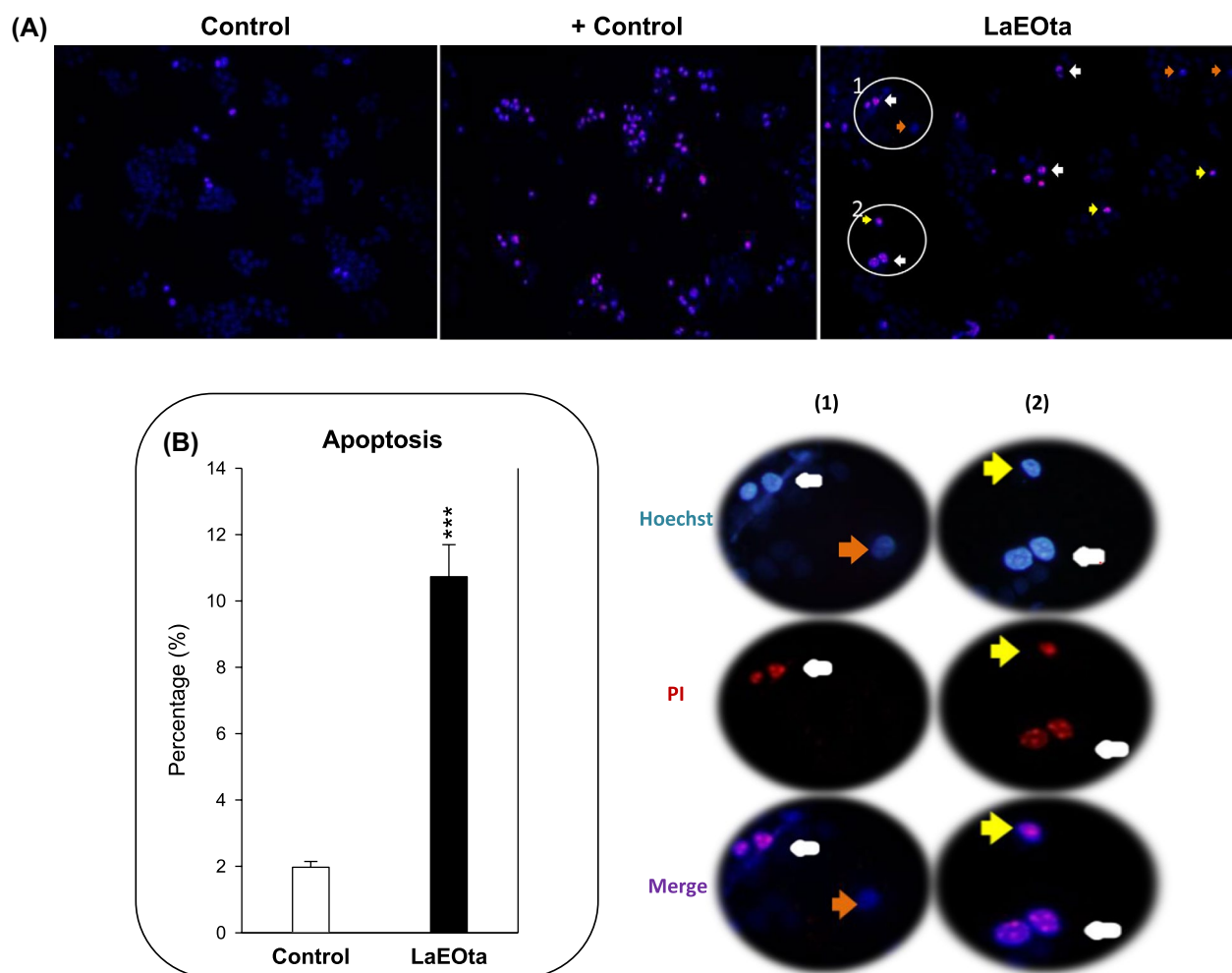


**Figure 4.** Cytological assay of the induction of apoptosis in HepG2 cells through Hoechst-33342–propidium-iodide double staining. Panel A: Representative composite photographic images of microscopical fields of HepG2 cells visualized by fluorescence microscopy (magnification 400×) revealed nuclear morphologic changes induced by LaEOta and detected through dual staining with Hoechst 33342 and PI. The cells shown had been treated with 0.2% (v/v) DMSO (Control), 3% (v/v) DMSO (+ Control) or 1.0× IC<sub>50</sub> LaEOta (LaEOta) for 48 h before being stained with the fluorescent dyes. Subfields (1) and (2) are magnified images of the regions indicated as 1 and 2 in Panel A. The arrows indicate: live cells with apoptotic nuclei (orange), dead cells with apoptotic nuclei (white) and dead cells with normal nuclei (yellow). Panel B: Percentages of apoptosis. The merge images from Panel A (blue and red fluorescence) of at least a total of 200 cells were analysed and classified according to the morphology of the Hoechst-33342–stained nuclei into normal or apoptotic cells and, depending on whether or not PI stained the nuclei, into to live or dead cells. The percentages of apoptotic cells were calculated as described in Materials and Methods. Values are the means ± SD, *n* = 4. \*\**p* < 0.01, \*\*\**p* < 0.001.

an increase in the number of cells positively labelled with TMR red through the TUNEL reaction, thus confirming that LaEOta induced apoptosis in both tumour cell lines (Figure 5 and Table 3).

### 3.6. Effect of LaEOta on the MP

We have previously proposed that EO-mediated growth suppression may be attributed to an inhibition of the MP. A quantification of the incorporation of radioactivity was used to determine the extent to which [<sup>14</sup>C]acetate was metabolized to cholesterol and other nonsaponifiable lipids of the MP (for example, lanosterol, squalene, dolicol,

and ubiquinone) after incubating the cells with 1.0× IC<sub>50</sub> of LaEOta for 48 h.

In the HepG2 cells (Figure 6(A)), the incorporation of acetate into squalene and lanosterol (MP intermediates specifically involved in cholesterol synthesis) and into ubiquinone (another final product of the MP besides cholesterol) could be readily quantified. The exposure to LaEOta inhibited cholesterologenesis by about 90% and decreased the incorporation of radioactivity into lanosterol (by 70%) and squalene (by 80%), whereas the incorporation into ubiquinone became increased (by about fourfold).

In the A549 cells (Figure 6(B)), the incorporation of [<sup>14</sup>C]acetate into only cholesterol, lanosterol and

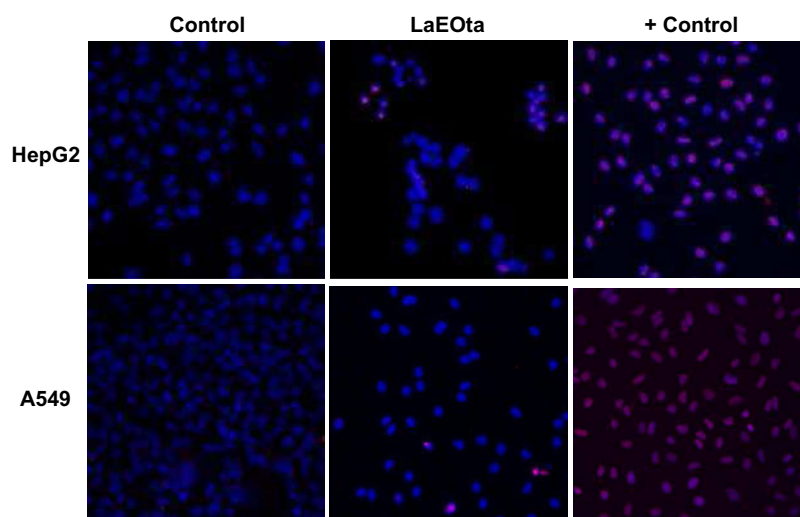


**Figure 5.** Representative fluorescence photomicrographs (40 $\times$ ) of some fields of HepG2 and A549 cells showing LaEOta-induced apoptosis as measured by the TUNEL reaction. Cells incubated without EO, then fixed and treated with DNAase for 30 min before the TUNEL assay were used as a positive control for the TMR-red labelling of free 3'-hydroxyl groups in the TUNEL reaction (+ Control). The apoptotic cells with TMR red fluorescence indicate DNA breakage in contrast to the nonapoptotic nuclei stained with DAPI alone.

**Table 3.** Induction of apoptosis in HepG2 and A549 cells by LaEOta as determined by the TUNEL assay.

	% Apoptotic cells	
	Hep G2	A549
Control	0.57 $\pm$ 0.14	1.67 $\pm$ 0.57
1.0 $\times$ IC <sub>50</sub>	9.38 $\pm$ 1.35**	6.32 $\pm$ 3.34 **

Notes: The TUNEL-positive cells were counted in 10 random fields with 300 cells/field under each experimental condition. The values are the means  $\pm$  SD,  $n = 4$ .

\*\* $p < 0.01$ .

ubiquinone could be quantified; whereas squalene and other MP intermediates and final products remained undetectable under these treatment conditions. LaEOta decreased the incorporation of radioactivity into cholesterol and lanosterol by about 90%, but the ubiquinone labelling was greatly increased (by about 25-fold).

Despite this profound inhibition of cholesterol synthesis, cholesterol content in the two cell types remained unchanged (data not shown).

### 3.7. Effect of LaEOta on HMGCR

In order to determine if the antiproliferative effects were associated with a downregulation of HMGCR, we treated HepG2 cells with 0.5 $\times$  and 1 $\times$  IC<sub>50</sub> of LaEOta for 48 h and determined HMGCR protein levels by Western blotting. The results indicated that LaEOta reduced HMGCR levels in a concentration-dependent manner (Figure 7).

### 3.8. Effect of mevalonate (Mv) addition on the inhibition of cell viability induced by LaEOta

To determine whether HMGCR inhibition was the cause or the result of LaEOta-induced tumour cell cytotoxicity,

we treated HepG2 and A549 cells with increasing concentrations of LaEOta (0.5 $\times$ , 1.0 $\times$ , and 1.75 $\times$  IC<sub>50</sub>), or with Sv with or without mevalonate (Mv; 0.5 mM) for 48 h, then measured cellular viability by the MTT assay. The competitive inhibitor of HMGCR Sv, at the indicated concentrations, was employed as a positive control for the possibility of a reduced cell growth that could then be restored by the addition of Mv. When added to the culture medium, though, Mv did not reverse the decrease in viability caused by the LaEOta concentrations tested. Exogenous Mv, however, as expected, significantly restored cell viability in the Sv-treated cells (Table 4).

## 4. Discussion

The study of natural products has been the single most successful strategy for the discovery of new medicines used in anticancer therapy (2,3). In the work presented here, we initially assessed the potential pharmacologic utility in cancer therapy of EOs extracted from four *L. alba* chemotypes (carvone, piperitone, tagetenone, and citral) cultivated in Costa Rica. One of the parameters to consider in the selection of potential antitumour drugs is their effectiveness in inhibiting tumour cell growth. Therefore, in order to analyse the cytotoxicity of the four LaEO chemotypes in tumour cells, we evaluated the effect on cell viability.

The National Cancer Institute of the USA (US-NCI) established that a crude extract that shows an IC<sub>50</sub> value of less than 100  $\mu$ g/mL should be considered cytotoxically active. When the IC<sub>50</sub> value is lower than 30  $\mu$ g/mL, the US-NCI considers such an extract promising for purification and a study of the biologic activity (30).

The assays reported here indicated that 50% inhibition of viability was obtained with concentrations near 30  $\mu$ g/mL

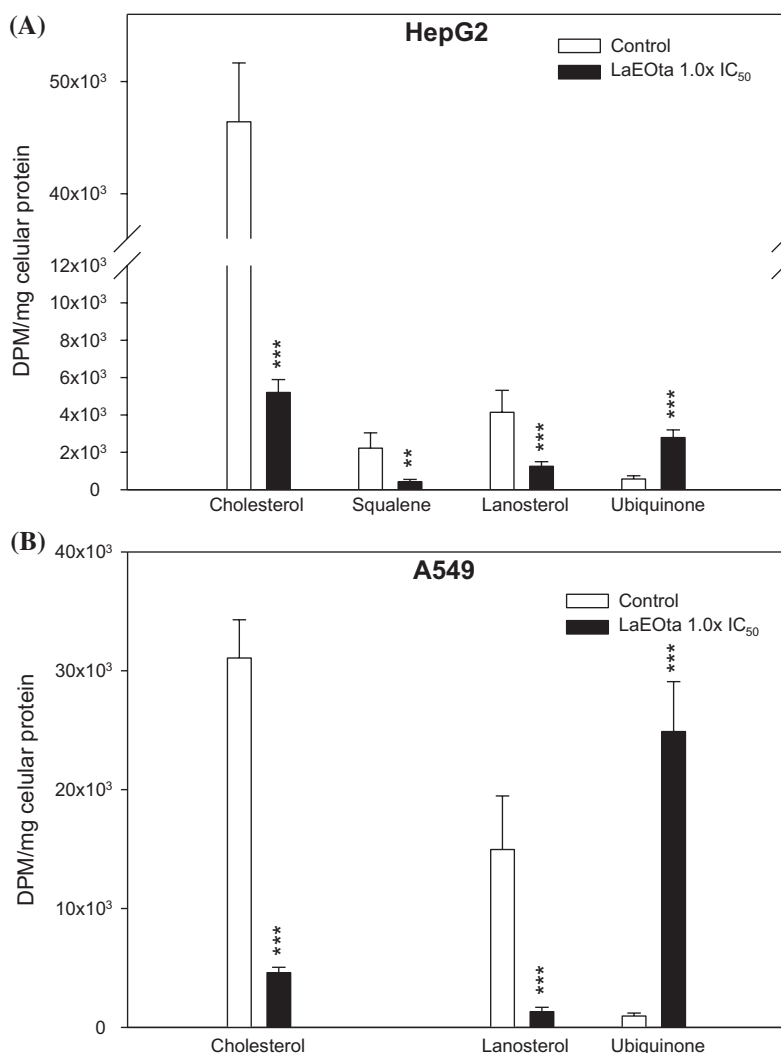


**Figure 6.** [<sup>14</sup>C]acetate incorporation into cholesterol and other nonsaponifiable lipids of the mevalonate pathway in HepG2 and A549 cells. The incorporation of radioactivity into cholesterol, lanosterol, squalene, and ubiquinone in HepG2 cells (Panel A) and into cholesterol, lanosterol and ubiquinone in A549 cells (Panel B) was located by autoradiography and quantitated by densitometric analysis. The data are expressed as the means  $\pm$  SD ( $n = 4$ ); \* $p < 0.05$ , \*\* $p < 0.01$ , \*\*\* $p < 0.001$ .

for the A549 and HepG2 cells with the LaEOs of tagetenone and citral chemotypes (Table 2). The IC<sub>50</sub> values obtained for A549 and HepG2 cells treated with the LaEOs of carvone and piperitone chemotypes failed to classify as cytotoxic crude extracts by the US-NCI criteria. For the IC<sub>50</sub> values in Vero cells, LaEOs carvone, piperitone and tagetenone chemotypes showed little or no cytotoxicity, and only the citral chemotype could be considered cytotoxically active in this nontumour cell line.

Another parameter to consider in the screening of anticancer drugs is the selectivity of the cytotoxicity on tumour cells compared to nontumour cells. According to the criteria used by Bézivin et al. (2003), the selectivity index (SI) is of interest when values are greater than 3. In the present work, the only LaEO that was highly selective for tumour cells was the tagetenone chemotype with an SI near to 7 (Table 2). Moreover, concentrations

of this chemotype that exhibited a strong cytotoxicity to the carcinoma cell lines (at more than a 95% inhibition of viability) did not significantly affect the noncancerous cell line (Figure 1). Therefore, because LaEOta manifests both a marked cytotoxicity and a strong selectivity for cancerous cells, this EO represents a promising anticancer phytochemical to be evaluated in pre-clinical tests.

The cytotoxicity and selectivity of various *Lippia*-genus EOs have been analysed by other authors, but with variable results (11,22,23). To the best of our knowledge, this present communication constitutes the first evaluation of the LaEO tagetenone chemotype.

The different biologic activities of the various types and chemotypes of EOs have been attributed mainly to differences in the composition of the constituent monoterpenes, those being considered primarily responsible for the antitumour activity when present (11,12,22).

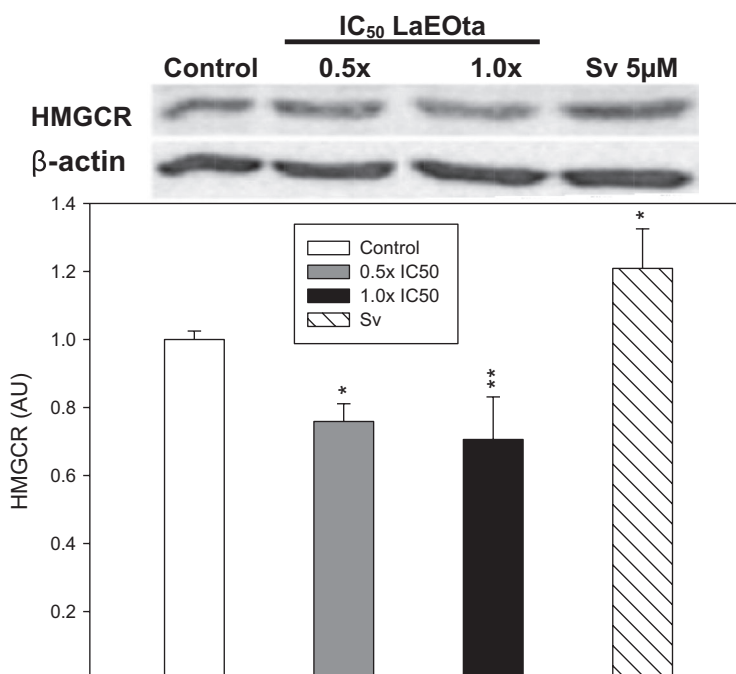


**Figure 7.** Effect of LaEOta on HMGCR protein levels in HepG2 cells. Cells in exponential growth were treated with 0.5× and 1.0× IC<sub>50</sub> of LaEOta. Simvastatin (Sv) at 5 µM was employed as a positive control for increased HMGCR levels. The results are expressed as corrected band density relative to that of the control. Data are expressed as the means ± SD ( $n = 3$ ); \* $p < 0.05$ , \*\* $p < 0.01$ , \*\*\* $p < 0.001$ . AU, arbitrary units.

**Table 4.** Failure to prevent the decrease in cell viability in HepG2 and A549 cells caused by essential oil tagetenona chemotypes from *Lippia alba* (LaEOta) through the addition of exogenous mevalonate.

	HepG2		A549	
	-Mv	+Mv	-Mv	+Mv
Control	100.00 ± 2.93	109.00 ± 10.84	100.00 ± 3.16	110.00 ± 6.18
0.5× IC <sub>50</sub> LaEO	78.64 ± 7.22	78.59 ± 7.58	82.91 ± 0.59	74.89 ± 5.49
1.0× IC <sub>50</sub> LaEO	41.64 ± 6.29	38.85 ± 1.46	54.93 ± 2.96	61.52 ± 3.37
1.75× IC <sub>50</sub> LaEO	15.39 ± 4.94	14.09 ± 0.97	30.59 ± 1.27	36.15 ± 2.72
Sv 10 µM	77.78 ± 3.05	123.16 ± 2.70***	nd	nd
Sv 20 µM	nd	nd	60.13 ± 1.61	98.68 ± 4.92***

Notes: Cell viability was determined by the MTT assay and the results expressed as a per cent of the control values. The data are the means ± SD ( $n = 4$ ). nd, not determined.

\* $p < 0.05$ , \*\* $p < 0.01$ , \*\*\* $p < 0.001$  vs. the same treatment without Mv.

We recently reported that the 1,8-cineole, one of the principal monoterpenes of LaEOta, inhibited the viability of HepG2 and A549 cells (27). The IC<sub>50</sub> values registered for 1,8-cineole with the two cell lines (6,050 µM = 933 µg/mL and 5030 µM = 776 µg/mL, respectively) were much higher than those found here for LaEOta. This difference would be consistent with the findings of several authors and is attributed to increased activity of the main components through an additive or synergistic interaction with

one or more of the other components in the complete EO (31,32). Therefore, studies on individual ingredients might report results that do not reproduce the effect of treatment with the phytochemical as a whole.

While the selectivity and cytotoxicity of the EOs is well documented in screening studies, the mechanisms underlying these effects have been very little explored. Different mechanisms may account for the reported cytotoxicities of EOs or their constituents (9).

Cell cycle arrest is a common cause of the growth inhibition of cell populations and is one of the mechanisms through which EOs can exercise their cytotoxicity (9). We show here that LaEOta cytotoxicity to HepG2 and A549 cells is linked to an inhibition of proliferation as a result of cell cycle arrest (Figure 3). Cytostatic effects with arrests at both G1 and G2 have been reported for other essential oils and monoterpenes (11,33).

The induction of apoptosis, an event accompanying cell cycle arrest in isoprenoid-induced growth suppression, is another mechanism through which EOs can exert their cytotoxicity (9), whose action is considered a valuable asset in cancer therapies.

In this work, we have demonstrated that LaEOta is able to induce alterations in nuclear morphology and DNA fragmentation in HepG2 and A549 tumour cells (Figures 4 and 5, Table 3), characteristic stages of cell death effected through apoptosis. Thus, the anticancer mechanism of



LaEOta on HepG2 and A549 cells would appear to involve the induction of apoptosis.

Cell cycle arrest and the proapoptotic effects of EOs have been attributed to interference by the principal constituents with multiple biochemical processes linked to cell growth and proliferation (9). With respect to the latter functions, the antiproliferative activity of monoterpenes has been attributed to multiple inhibitory effects on the MP. Certain terpenoids inhibit HMGCR by decreasing the amount of enzyme. In HepG2 cells exposed to linalool, Cho et al. (34) reported a decrease in HMGCR levels caused by an inhibition at the transcriptional level along with an increased degradation of the enzyme, while we more recently demonstrated that geraniol inhibited HMGCR at a post-transcriptional step (14).

In this study we have shown that a concentration of LaEOta that inhibits cell viability by 50% also leads to decreased HMGCR levels in HepG2 cells (Figure 7). HMGCR inhibition, in turn, decreases the synthesis of end products (cholesterol, ubiquinone, and dolichol) that perform fundamental physiologic functions and prevents the small GTPase Ras translocation and the subsequent activation downstream of the mitogen-activated and extracellular signal-regulated protein kinases MEK/ERK and PI3 K/Akt regulatory signalling cascades, leading to an inhibition of cell cycle progression and apoptosis in cancer cells (35,36). Under these conditions, however, the addition of Mv does not reverse the decrease in viability occasioned by LaEOta; thus, an inhibition of the reductase cannot be the cause of the cytotoxicity exerted by this EO (Table 4).

We have also shown that experimental conditions in which HMGCR levels are decreased result in a profound inhibition of cholesterologenesis (90%) and of acetate incorporation into intermediates of the MP specifically linked to sterol formation, but those same conditions caused an increase in the synthesis of other end products of the pathway (for example, ubiquinone, Figure 6). Thus, the decline in cholesterol synthesis would be attributable to an inhibition of HMGCR in addition to a blockade at some other step(s) of the MP along the direct pathway to cholesterol – presumably the conversion of FPP to squalene by squalene synthetase. Further data will be required to confirm which enzyme in that segment of the MP is inhibited.

Despite the decrease in the HMGCR levels, under our experimental conditions, the inhibition of cholesterologenesis-specific steps was strong enough to cause an accumulation and redirection of FPP (metabolite at the main branch point of the MP) into the generation of other final products of the MP such as ubiquinone. Similar effects have been reported for monoterpenes such as linalool and 1,8-cineole in HepG2 and A549 cells (27) or geraniol in HepG2 cells (16).

Although cholesterologenesis is profoundly inhibited, the cellular cholesterol content is preserved probably because the cells were able to meet their cholesterol requirement through the uptake of exogenous sterol from the serum in the medium, as we previously reported for HepG2 cells treated with the monoterpene geraniol (16). Therefore, the inhibition of cholesterol synthesis would appear not to be the cause of the antiproliferative effect of LaEOta.

Certain monoterpenoids contained in EOs compete with protein isoprenylation reactions by slowing down or blocking the function of cellular signalling proteins that lead to the growth of cancer cells (37–39). Many EO constituents inhibit Ras-family isoprenylation and thereby block the development of cancer. Such was found to be the action of limonene (37,40) and perillyl alcohol (35). Further studies are required to elucidate whether or not an inhibition of protein prenylation is linked to the cytotoxicity exerted by this EO.

In conclusion, LaEOta exhibited significant cytotoxicity against human hepatic and pulmonary carcinoma cells and showed potential selectivity towards malignant cells. Cytotoxic mechanism of LaEOta with HepG2 and A549 cells involved cell cycle arrest and apoptosis induction.

## Acknowledgements

We would like to thank Dr. Donald F. Haggerty, a retired academic career investigator and native English speaker, for editing the final version of the manuscript.

## Disclosure statement

No potential conflict of interest was reported by the authors.

## Funding

This work was supported by Agencia Nacional de Promoción Científica y Tecnológica, Argentina [grant number PICT-2007-00762]; Universidad Nacional de La Plata [grant number 11/M174].

## References

1. WHO, *World Cancer Report*. Edits., B.W. Stewart and C.P. Wild, p. 630, WHO Press Ed., IARC Nonserial, Geneva (2014).
2. X. Ma and Z. Wang, *Anticancer drug discovery in the future: an evolutionary perspective*. *Drug Discov. Today*, **14**, 1136–1142 (2009).
3. E. Turrini, L. Ferruzzi and C. Fimognari, *Natural compounds to overcome cancer chemoresistance: toxicological and clinical issues*. *Expert Opin. Drug Met.*, **10**, 1677–1690 (2014).
4. F. Bakkali, S. Averbeck and M. Idaomar, *Biological effects of essential oils – a review*. *Food Chem. Toxicol.*, **46**, 446–475 (2008).

5. D.P. de Sousa (ed.), *Medicinal essential oils: chemical, pharmacological and therapeutic aspects*. Nova Sci. Publ., New York, NY (2012).
6. A.E. Edris, Pharmaceutical and therapeutic Potentials of essential oils and their individual volatile constituents: a review. *Phytother. Res.*, **21**, 308–323 (2007).
7. B. Bayala, I.H.N. Bassole, R. Scifo, C. Gnoula, L. Morel, J.-M.A. Lobaccaro and J. Simpoire, *Anticancer activity of essential oils and their chemical components-a review*. *Am. J. Cancer Res.*, **4**, 591–607 (2014).
8. N. Gautam, A.K. Mantha and S. Mittal, *Essential oils and their constituents as anticancer agents: a mechanistic view*. *Biomed Res. Int.*, **2014**, 154106 (2014).
9. J.F. Lesgards, N. Baldovini, N. Vidal and S. Pietri, Anticancer activities of essential oils constituents and synergy with conventional therapies: a review. *Phytother. Res.*, **28**, 1423–1446 (2014).
10. S. Patel and P. Gogna, *Tapping botanicals for essential oils: Progress and hurdles in cancer mitigation*. *Ind. Crop. Prod.*, **76**, 1148–1163 (2015).
11. R.P. Ferraz, D.S. Bomfim, N.C. Carvalho, M.B. Soares, T.B. da Silva, W.J. Machado, A.P.N. Prata, E.V. Costa, V.R.S. Moraes and P.C.L. Nogueira, *Cytotoxic effect of leaf essential oil of Lippia gracilis Schauer (Verbenaceae)*. *Phytomedicine*, **20**, 615–621 (2013).
12. M.V. Sobral, A.L. Xavier, T.C. Lima and D.P. de Sousa, *Antitumor activity of monoterpenes found in essential oils*. *Sci. World J.*, **2014**, (2014).
13. M.T. Cardozo, A. de Conti, T.P. Ong, C. Scolastici, E. Purgatto, M.A. Horst, B.K. Bassoli and F.S. Moreno, *Chemopreventive effects of  $\beta$ -ionone and geraniol during rat hepatocarcinogenesis promotion: distinct actions on cell proliferation, apoptosis, HMGCoA reductase, and RhoA*. *J. Nutr. Biochem.*, **22**, 130–135 (2011).
14. R. Crespo, S. Montero Villegas, M.C. Abba, M.G. de Bravo and M.P. Polo, *Transcriptional and posttranscriptional inhibition of HMGCR and PC biosynthesis by geraniol in 2 Hep-G2 cell proliferation linked pathways*. *Biochem. Cell Biol.*, **91**, 131–139 (2013).
15. M. Pattanayak, P.K. Seth, S. Smita and S.K. Gupta, *Geraniol and Limonene Interaction with 3-hydroxy-3-methylglutaryl-CoA (HMG-CoA) Reductase for their Role as Cancer Chemo-preventive Agents*. *J. Proteomics Bioinf.*, **2**, 466–474 (2009).
16. M.P. Polo and M.G. de Bravo, *Effect of geraniol on fatty acid and mevalonate metabolism in the human hepatoma cell line Hep G2*. *Biochem. Cell Biol.*, **84**, 102–111 (2006).
17. J.L. Goldstein and M.S. Brown, *Regulation of the mevalonate pathway*. *Nature*, **343**, 425–430 (1990).
18. M. Wang and P.J. Casey, *Protein prenylation: unique fats make their mark on biology*. *Nat. Rev. Mol. Cell Bio.*, **17**, 110–122 (2016).
19. J.F. Cicció and R. Ocampo, *Distribución biogeográfica de Lippia alba (Mill.) NE Br. ex Britton & Wilson y quimiotipos en América y el Caribe*. In: *Normalización de productos naturales obtenidos de especies de la flora aromática Latinoamericana*. Edit., E. Dellacassa, pp. 107–130, EdiPUCRS, Porto Alegre, Brazil (2010).
20. T. Hennebelle, S. Sahpaz, H. Joseph and F. Bailleul, *Ethnopharmacology of Lippia alba*. *J. Ethnopharmacol.*, **116**, 211–222 (2008).
21. G. Ricciardi, J.F. Cicció, R. Ocampo, D. Lorenzo, A. Ricciardi, A. Bandoni and E. Dellacassa, *Chemical variability of essential oils of Lippia alba (Miller) N.E. Brown growing in Costa Rica and Argentina*. *Nat. Prod. Commun.*, **4**, 853–858 (2009).
22. A.C. Mesa-Arango, J. Montiel-Ramos, B. Zapata, C. Durán, L. Betancur-Galvis and E. Stashenko, *Citral and carvone chemotypes from the essential oils of Colombian Lippia alba (Mill.) NE Brown: composition, cytotoxicity and antifungal activity*. *Mem. I. Oswaldo Cruz*, **104**, 878–884 (2009).
23. B. Zapata, L. Betancur-Galvis, C. Duran and E. Stashenko, *Cytotoxic activity of Asteraceae and Verbenaceae family essential oils*. *J. Essent. Oil Res.*, **26**, 50–57 (2014).
24. C. Chaverri and J.F. Cicció, *Leaf and fruit essential oil compositions of Pimenta guatemalensis (Myrtaceae) from Costa Rica*. *Rev. Biol. Trop.*, **63**, 303–311 (2015).
25. H. van Den Dool and P.D. Kratz, *A generalization of the retention index system including linear temperature programmed gas – liquid partition chromatography*. *J. Chromatogr. A*, **11**, 463–471 (1963).
26. R.P. Adams, *Identification of essential oil components by gas chromatography/mass spectrometry*, 4th ed., Allured Publ. Corp, Carol Stream, IL (2007).
27. B.R. Kladniew, M. Polo, S.M. Villegas, M. Galle, R. Crespo and M.G. de Bravo, *Synergistic antiproliferative and anticholesterogenic effects of linalool, 1,8-cineole, and simvastatin on human cell lines*. *Chem.-Biol. Interact.*, **214**, 57–68 (2014).
28. C. Bézivin, S. Tomasi and F. Lohézic-Le, *Dévêhat and J. Boustie, Cytotoxic activity of some lichen extracts on murine and human cancer cell lines*. *Phytomedicine*, **10**, 499–503 (2003).
29. S.N. Syed Abdul Rahman, N. Abdul Wahab and S.N. Abd Malek, *In vitro morphological assessment of apoptosis induced by antiproliferative constituents from the rhizomes of Curcuma zedoaria*. *Evid-Based Compl. Alt.*, **2013**: art. ID 257108 (2013).
30. M. Suffness and J.M. Pezzuto, *Assays related to cancer drug discovery*. In: *Methods in plant biochemistry: Assays for bioactivity*. Edit., K. Hostettmann, **6**, 71–133, Academic Press, London (1990).
31. R. Russo, A. Ciociaro, L. Berliocchi, M.G. Cassiano, L. Rombolà, S. Ragusa, G. Bagetta, F. Blandini and M.T. Corasaniti, *Implication of limonene and linalyl acetate in cytotoxicity induced by bergamot essential oil in human neuroblastoma cells*. *Fitoterapia*, **89**, 48–57 (2013).
32. R. Russo, M.T. Corasaniti, G. Bagetta and L.A. Morrone, *Exploitation of cytotoxicity of some essential oils for translation in cancer therapy*. *Evid-Based Compl. Alt.*, **2015**: art.ID397821 (2015).
33. W. Chen, Y. Liu, M. Li, J. Mao, L. Zhang, R. Huang, X. Jin and L. Ye, *Anti-tumor effect of  $\alpha$ -pinene on human hepatoma cell lines through inducing G2/M cell cycle arrest*. *J. Pharmacol. Sci.*, **127**, 332–338 (2005).
34. S.-Y. Cho, H.-J. Jun, J.H. Lee, Y. Jia, K.H. Kim and S.-J. Lee, *Linalool reduces the expression of 3-hydroxy-3-methylglutaryl CoA reductase via sterol regulatory element binding protein-2-and ubiquitin-dependent mechanisms*. *FEBS Lett.*, **585**, 3289–3296 (2011).
35. S. Afshordel, B. Kern, J. Clasohm, H. Konig, M. Priester, J. Weissenberger, D. Kogel and G.P. Eckert, *Lovastatin and perillyl alcohol inhibit glioma cell invasion, migration,*

- and proliferation – Impact of Ras-/Rho-prenylation. *Pharmacol. Res.*, **91**, 69–77 (2015).
36. C.-C. Chen, M.-L. Wu, C.-T. Ho and T.-C. Huang, Blockade of the Ras/Raf/ERK and Ras/PI3K/Akt Pathways by Monacolin K Reduces the Expression of GLO1 and Induces Apoptosis in U937 Cells. *J. Agr. Food Chem.*, **63**, 1186–1195 (2015).
37. M.N. Gould, C.J. Moore, R. Zhang, B. Wang, W.S. Kennan and J.D. Haag, *Limonene chemoprevention of mammary carcinoma induction following direct in situ transfer of v-Ha-ras*. *Cancer res.*, **54**, 3540–3543 (1994).
38. H. Loza-Tavera, *Monoterpenes in essential oils. Biosynthesis and properties*. *Adv. Exp. Med. Biol.*, **464**, 49–62 (1999).
39. M.N. Gould, *Cancer chemoprevention and therapy by monoterpenes*. *Environ. Health Perspect.*, **105**, 977–979 (1997).
40. S.C. Chaudhary, M.S. Siddiqui, M. Athar and M.S. Alam, d-Limonene modulates inflammation, oxidative stress and Ras-ERK pathway to inhibit murine skin tumorigenesis. *Hum. Exp. Toxicol.*, **31**, 798–811 (2012).